Investigation on performance of special-shaped 8-quadrature amplitude modulation constellations applied in visible light communication

Jiaqi Zhao, Chaoyi Qin, Mengjie Zhang, and Nan Chi*

Key Laboratory for Information Science of Electromagnetic Waves (MoE), Department of Communication Science and Engineering, Fudan University, Shanghai 200433, China
**Corresponding author: nanchi@fudan.edu.cn*

Received June 27, 2016; revised August 23, 2016; accepted September 9, 2016; posted September 9, 2016 (Doc. ID 268985); published October 20, 2016

Light-emitting diode (LED)-based visible light communication (VLC) has become a potential candidate for next-generation ultra-high-speed indoor wireless communication. In this paper, four special-shaped 8-quadrature amplitude modulation (QAM) constellations are investigated in a single-carrier VLC system. It is numerically verified and experimentally demonstrated that circular (7,1) shows obvious superiority in the performance of the dynamic range of signal voltage peak-to-peak (vpp) value and bit error rate (BER). Next best is rectangular, followed by triangular; circular (4,4) has the worst performance. A data rate of 1.515 Gbit/s is successfully achieved by circular (7,1) employing a red chip LED over 0.5 m indoor free space transmission below a BER threshold of 3.8×10^{-3}. Compared with circular (4,4), the traditional 8-QAM constellation, circular (7,1) provides a wider dynamic range of signal vpp, a higher data rate, and a longer transmission distance. To the best of our knowledge, this is the first investigation into the performance differences of special-shaped 8-QAM constellations in a high-speed, single-carrier VLC system, and the results comprehensively demonstrate that circular (7,1) is the optimal option.

OCIS codes: (060.2605) Free-space optical communication; (060.4510) Optical communications; (230.3670) Light-emitting diodes.
http://dx.doi.org/10.1364/PRJ.4.000249

1. INTRODUCTION

Visible light communication (VLC) is an emerging wireless communication technology utilizing visible light as the medium to deliver information. In VLC systems, signals are modulated onto high-performance light-emitting diodes (LEDs), which realize the dual function of lighting and communication. Compared with traditional wireless communication at radio frequency (RF), VLC shows several advantages, including high efficiency, high security, free spectrum license, and immunity to electromagnetic interference. Therefore, VLC has attracted growing attention and become a worldwide hotspot [1,2].

Furthermore, the unique advantages of VLC have brought about various emerging applications, such as localization, screen–camera communication, vehicular communication, and human–computer interaction (HCI). Take indoor localization as an example. VLC is superior to wireless fidelity in terms of the number of access points, thus providing higher localization accuracy. In the numerical analysis of [3], the estimation error of detecting could be achieved as low as ~5 cm with a detection range of up to ~6 m. Screen–camera communication is another typical example where VLC-based screen–camera links are highly directional, low interference, and secure due to the short wavelengths and narrow beams of visible light [4]. However, noise from ambient light, high-frequency attenuation of LED response, and the nonlinear effect have restricted service conditions. This paper is dedicated to finding a more flexible modulation technique to support these various applications. As one of the main research directions of high-order quadrature amplitude modulation (QAM) techniques, the constellation-shaping scheme is the main research content of this paper.

The constellation-shaping scheme has been extensively studied and employed. References [5,6] provided early theoretical studies on the design of digital M-QAM constellation shaping. References [7–9] employed constellation-shaping schemes for peak-to-average power ratio (PAPR) reduction. References [10,11] investigated the combination of constellation shaping with bit-interleaved coded modulation. VLC is a communication technology that originated in 2000. Though the past few decades have witnessed their rapid development in scientific research, there has been no systematic research achievement in the application of constellation-shaping schemes. In this paper, we make a preliminary study on constellation-shaping schemes appropriate for indoor VLC systems. Higher order QAM has higher spectral efficiency, but it requires a higher signal-to-noise ratio (SNR). However, because the received power of commercial LEDs is limited due to the path loss and the relatively big divergence angle, the received SNR is limited. As a compromise of spectral efficiency and SNR, 8-QAM is an appropriate option to be researched in VLC systems.

For 8-QAM constellation shaping, Thomas performed a theoretical analysis on the performance of four possible special-shaped 8-QAM constellations [5], shown in Fig. 1. The main design principle was to equably allocate the constellation points into circles, regular triangles, squares, or other

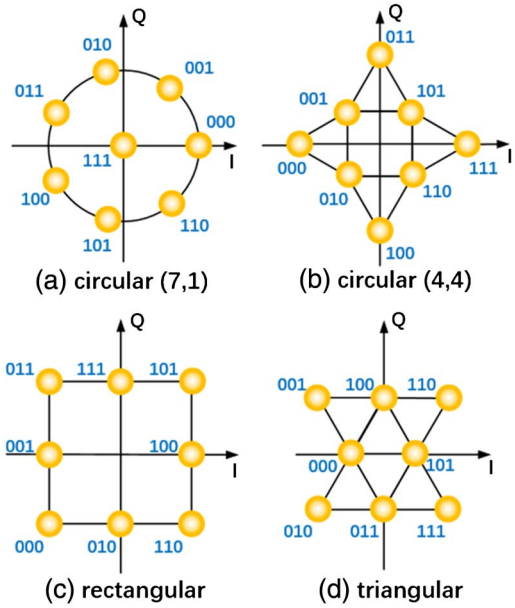

Fig. 1. 8-QAM constellation design.

regular polygons. In Thomas's research, he only considered the additive white Gaussian noise (AWGN) channel and found circular (7,1) performed best. Based on Thomas's work, Nölle *et al.* carried out a further study, considering a more complex channel in the application of flexible optical fiber communications [12]. They made a comparison of the first three constellations, as shown in Fig. 1, and experimentally demonstrated that circular (7,1) was still the best. However, they didn't provide any theoretical explanations for why such constellation shaping performs better under the certain channel of optical fiber communication.

Thomas *et al.* conducted research on 8-QAM constellation schemes in a single-carrier system [5,12]. Based on their works, we conduct numerical and experimental comparisons of the four special-shaped constellations in a certain channel of a single-carrier VLC system. The results show that circular (7,1) outperforms the other three constellations with its larger minimum Euclidean distance and lower PAPR, while the performance of circular (4,4), the most widely used 8-QAM, is the worst. In addition, the dynamic range of the signal voltage peak-to-peak (vpp) of circular (7,1) is much wider than that of other constellations, which supports its application in a more complicated environment. From a particular comparison between circular (7,1) and circular (4,4), a Q-factor improvement of 4.5 dB at 500 MBd is achieved by circular (7,1) under the bit error rate (BER) threshold of 3.8×10^{-3}. Besides, circular (7,1) increases the highest data rate by 105 Mbit/s. At the baud rate of 470 MBd, the transmission distance is also increased by 1.5 m.

To the best of our knowledge, it is the first time the performance differences of special-shaped 8-QAM constellations in VLC systems have been investigated. The results demonstrate the feasibility and superiority of circular (7,1) and indicate the scientific research value of constellation-shaping schemes in VLC.

The rest of the paper is organized as follows. Section 2 provides the numerical analysis of the four special-shaped 8-QAM constellations in terms of noise resistance, high-frequency attenuation resistance, and nonlinearity resistance. In Section 3, we describe the setup of the corresponded experiment. Then we analyze and discuss the experimental results in Section 4. Based on the numerical analysis and experiment results, we finally come to the conclusion in Section 5.

2. NUMERICAL ANALYSIS

In this section, we numerically analyze the performance of the four special-shaped 8-QAM constellations in terms of noise resistance, high-frequency attenuation resistance, and nonlinearity resistance. Noise-resistant ability is a fundamental criterion of the constellation evaluation. There are three major sources of noise in the VLC link: (1) shot noise from photoelectric detectors and ambient light, (2) thermal noise induced by amplifiers, and (3) background noise generalized by ambient light [4]. LED frequency response usually shows high-frequency attenuated characteristics due to the influence of response speed of carriers. Currently, the highest modulation bandwidth of commercial LEDs is only about 20–30 MHz, which is a great challenge for achieving high-speed VLC transmission. Thus, we compare the performance of the four constellations under high-frequency attenuation. Similar to RF communication, nonlinearity is also a limiting factor of VLC systems. And its influence is amplified because of the severer nonlinear relationship between driving voltage and forward current of LEDs. Therefore, the analysis of nonlinearity resistance is necessary.

A. Noise Resistance

In this section, the symbol decision is based on the most-adjacent principle, where the received symbol is judged as the nearest one in the constellation set. For a more rigorous mathematical perspective, consider the constellation S with eight points, or symbols, $S = [s_1, s_2, \ldots s_8]$. Each point has a decision region based on the Voronoi boundary [13]. That is to say, the error probability can be regarded as the probability of a point added with Gaussian noise outside its Voronoi boundary. A simple approximation to the symbol error rate (SER) is the union bound expressed as

$$\mathrm{SER} \le \frac{1}{M}\sum_{k=1}^{M}\sum_{j=1,j\neq k}^{M}\frac{1}{2}\,\mathrm{erfc}\left(\frac{d_{kj}}{2\sqrt{N_0}}\right), \tag{1}$$

where d_{kj} signifies the distance between the symbols s_k and s_j. N_0 is the noise variance.

According to Eq. (1), under the restriction of high SNR, the error probability is mainly dominated by the closest constellation points due to the term containing $\mathrm{erfc}\left(\frac{d_{\min}}{2\sqrt{N_0}}\right)$, where $d_{\min} = \min_{j\neq k} d_{kj}$ is the minimum Euclidean distance of the constellations.

The $d_{\min}$ values of the four special-shaped 8-QAM constellations have been calculated under normalized power. The results are listed in Table 1. Circular (7,1) has the biggest

Table 1. Minimum Euclidean Distances of Special-Shaped 8-QAM Constellations

Constellation	Min_Euclidean
Circular (7,1)	0.9277
Circular (4,4)	0.9194
Rectangular	0.8165
Triangular	0.8729

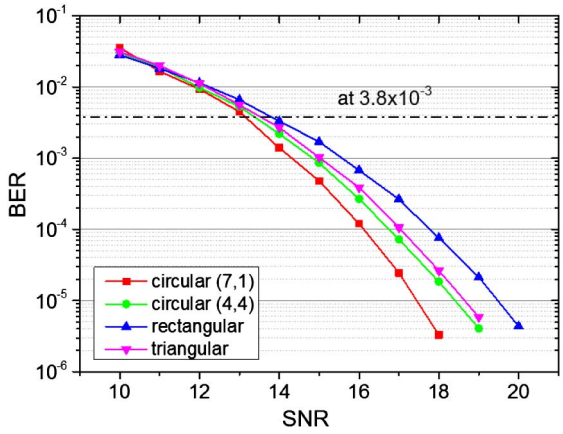

Fig. 2. BER versus average SNR.

$d_{\min}$, which indicates its superiority on the ability of noise immunity. Circular (4,4) comes in second and next are triangular and rectangular.

Figure 2 shows the simulation results of noise-resistance ability. The bit mapping schemes of the four constellations are as shown in Fig. 1. Only the rectangular is suitable for Gary mapping. Circular (7,1) and circular (4,4) are referred to in Ref. [12]. Though the results are in line with the minimum Euclidean distance analysis, the ability variance on the noise-resistant performance of the four constellations is not so obvious, especially around the BER threshold of 3.8×10^{-3}.

B. High-Frequency Attenuation Resistance

The limited modulation bandwidth of commercial LEDs is the main challenge of achieving high-speed VLC transmission. In this section, high-frequency attenuation is considered and analyzed.

The frequency response of a commercial white LED tested by pilot signals is shown in Fig. 3. It suffers serious high-frequency attenuation, and the bandwidth of –3 dB is only about 25 MHz. Frequency attenuation brings about intersymbol interference (ISI) and deteriorates communication quality.

The error probability under ISI is difficult to analyze. Bello and Nelin first made extensive analysis of ISI degradation with SER [14], where they only took the adjacent symbols into consideration. Though under the simplified condition, the expressions were too complex to be exactly represented. Therefore, SER performance with ISI is usually obtained by simulations and so is BER.

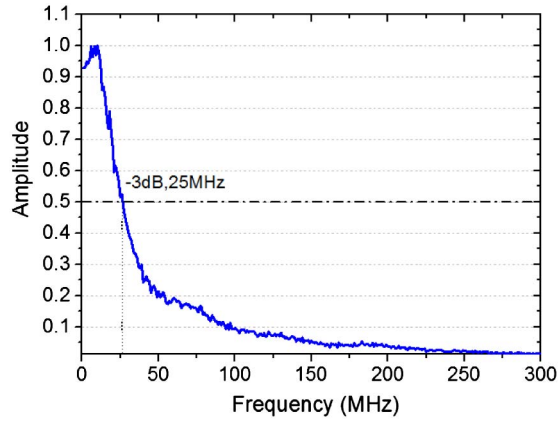

Fig. 3. Frequency response of a commercial LED.

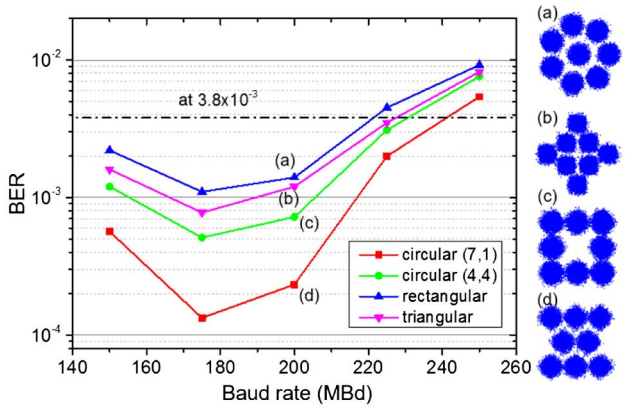

Fig. 4. BER versus baud rate under high-frequency attenuation.

Figure 4 shows the simulation results of high-frequency attenuation resistance, only considering the effect of the frequency response of the commercial LED. Because of the attenuation in low frequency shown in Fig. 3, the BER performance at 175 MBd is better than that at 150 MBd. As expected, circular (7,1) outperforms other constellations. It is worth noting that the gap between circular (7,1) and circular (4,4) is larger, and circular (7,1) shows more obvious advantages.

C. Nonlinearity Resistance

Similar to wireless communication systems at RF, VLC systems suffer signal distortions from nonlinear components. LEDs, digital-to-analog converters, electrical amplifiers (EAs), analog-to-digital converters, and photodiodes (PDs) are the main sources of nonlinearity [15].

Among all nonlinearities, the LEDs and PDs play dominant roles. The nonlinearity from PDs results from square-law detection, which is similar to typical optical fiber communication [16]. The nonlinearity from LEDs results from the nonlinear transform function. Figure 5 is the *U–I* curve of the red chip of an RGB–LED (LZ4-00MA00). The nonlinear relationship between driving voltage and forward current brings about two kinds of signal distortion. One is the nonlinear mapping in electrical-to-optical conversion within the dynamic range; the other is the hard clipping of signals when the voltage is under the turn-on voltage or above the maximum permissible voltage. Both of them may occur on large input

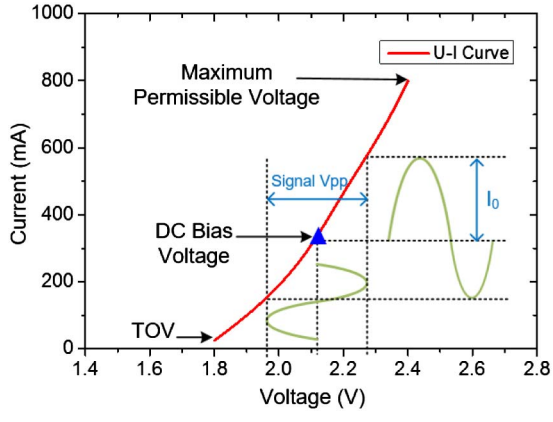

Fig. 5. *U–I* curve of the red chip of a commercial RGB–LED (LZ4-00MA00).

Table 2. PAPRs of Different Special-Shaped 8-QAM Constellations

Constellation	PAPR
Circular (7,1)	1.1429
Circular (4,4)	1.5774
Rectangular	1.3333
Triangular	1.5238

signals. Additionally, to increase the modulation depth defined as $m = \frac{I_0}{I_d}$, where I_d is the bias current and I_0 is the difference between peak current and bias current, I_0 needs to be comparable to I_d. Therefore, there is a tradeoff between nonlinearity and modulation depth. Constellations with low PAPR are more robust to nonlinear effects and obtain higher modulation depth.

Table 2 lists the PAPRs of the four special-shaped 8-QAM constellations. Circular (7,1) has the lowest PAPR among the four constellations. To provide a more practical analysis, we calculate the statistical distribution characteristics of signal peak with the aid of the complementary cumulative distribution function (CCDF), defined as the probability of PAPR exceeding a certain threshold. Figure 6 shows CCDF of PAPRs for the four special-shaped 8-QAM constellations in a single-carrier system. $PAPR_0$ represents the threshold. The results indicate that circular (7,1) has the lowest PAPR threshold compared with the other three constellations and is most robust to nonlinear effect. It is noted that the most common used circular (4,4) behaves poorly in PAPR performance, which means it is vulnerable to nonlinearities.

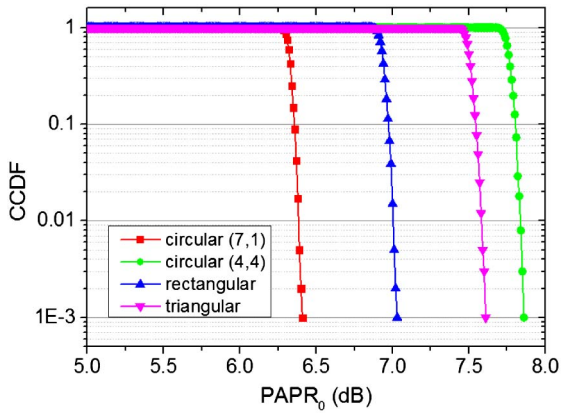

Fig. 6. CCDF of PAPRs for single-carrier, special-shaped 8-QAM signals.

According to the analysis results above, it is apparent that circular (7,1) performs best under VLC characteristic channels. Circular (4,4), the most widely used 8-QAM constellation due to its simple generation with an inphase/quadrature (IQ) modulator, is suboptimal in terms of noise resistance. Considering the effect of high-frequency attenuation, the performance difference between circular (7,1) and circular (4,4) is more obvious. What is more, circular (4,4) performs worse in nonlinear resistance because of high PAPR. It is reasonable to believe that circular (7,1) is more suitable than circular (4,4) for VLC systems. To verify the conclusion, we conducted a comparative experiment among the four special-shaped 8-QAM constellations.

3. EXPERIMENTAL SETUP

Figure 7 shows the experimental setup of a single-carrier special-shaped 8-QAM VLC system. At the transmitting end, the digital 8-QAM signal was produced by an offline MATLAB program and loaded into arbitrary waveform generator (AWG) (Tektronix AWG710) to generate the transmitted signal. The signal first passed through a hardware pre-equalizer to partially compensate the frequency attenuation at a high-frequency component [17]. Then the equalized signal was amplified by an EA (Minicircuits, 25 dB gain, 50 Ω input impedance, and 50 Ω output impedance) and coupled with direct current by a bias tee (ZX85-12G-S). The direct current was used to drive the RGB–LED (LZ4-00MA00) in the operation region. Finally, the electrical signal was converted into the optical signal by being modulated onto the red chip of the high-performance RGB–LED and transmitted through a free

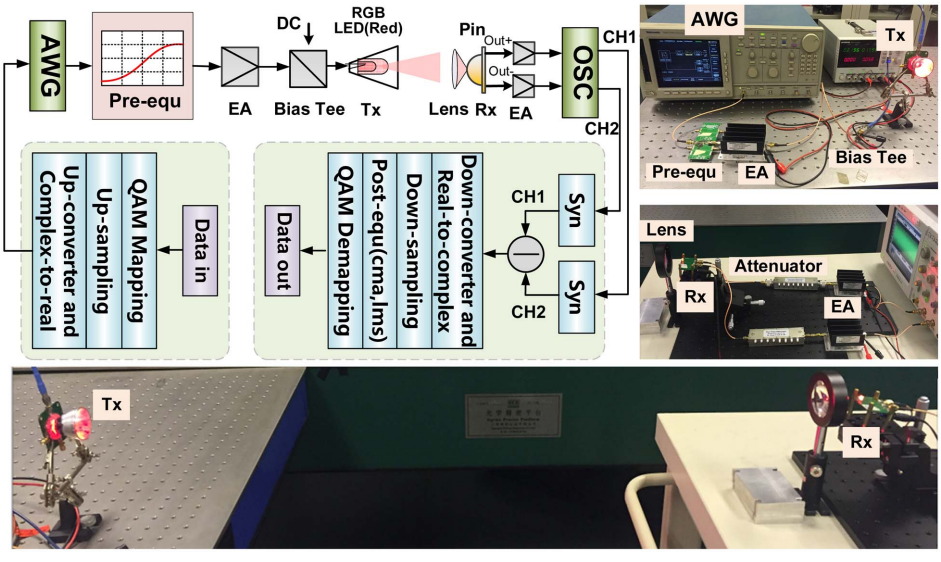

Fig. 7. Experimental setup of single-carrier, special-shaped 8-QAM VLC system.

space channel. Because commercial RGB–LEDs are usually point light sources, a reflection cup with 60° was used to concentrate light. At the receiving end, a commercial PIN PD (Hamamatsu 10784) that had a pair of differential outputs was utilized as the receiver to detect the signal and conduct photoelectric conversion. To achieve a higher received SNR, a lens (70 mm diameter and 100 mm focus length) was used to focus light. The two electrical signal streams from the differential outputs were amplified by EAs and recorded by a digital sampling oscilloscope (OSC, Agilent DSO54855A) through channel 1 (CH1) and channel 2 (CH2), respectively, for further offline digital signal processing (DSP).

For the offline signal generation at the transmitting end, the binary bit stream was first mapped onto the special-shaped 8-QAM symbols. Up-sampling was used to smooth the signal. In order to make the best use of bandwidth, while also preventing the spectrum from aliasing, five times up-sampling was adopted. Then the up-sampled signal was up-converted and became its equivalent real signal to be loaded into AWG.

For the offline DSP at the receiving end, differential signal from CH1 subtracted the signal from CH2 to partially suppress the noise. Because of device processing limitation, the differential outputs could not be absolutely symmetrical, and the improvement of differential reception was restricted. After a down-converter and real-to-complex module and a down-sampling module corresponded to the transmitting end, a constant modulus algorithm (CMA) and least mean square (LMS) algorithm were adopted for post equalization. CMA is one of the most common blind equalization algorithms; however, it is insensitive to phase error, so LMS was added for phase retrieval. Finally, the data was recovered by QAM demapping.

4. EXPERIMENTAL RESULTS AND DISCUSSION

First, we measured the BER performance under different bias voltage with different input signal vpps when the baud rate was 450 MBd and the transmission distance was 1 m. The results are shown in Fig. 8. Considering a BER threshold of 3.8×10^{-3} with 7% forward error correction (FEC), the operation range is circled by a black line. For all four special-shaped 8-QAM constellations, when the bias voltage is relatively lower or higher, the available range of signal vpp is smaller due to the severe *U–I* nonlinearity shown in Fig. 5. By comparing the area of operation range of the four constellations, we can obtain the result that circular (7,1) possesses the largest operation range; next is rectangular, triangular comes in third, and the operation range of circular (4,4) is the smallest, which is in line with the theoretical analysis of PAPR in Section 2.

For a more detailed comparison, we mapped out the relationship between BER performance and input signal vpp when the bias voltages were 1.8, 2.0, and 2.3 V. The results are shown in Figs. 9(a)–9(c). For a clearer illustration, the exact dynamic ranges of signal vpp for different constellations under 1.8, 2.0, and 2.3 V are listed in Table 3. As expected, circular (7,1) shows an obvious advantage in the dynamic range over three other constellations, and circular (4,4) shows the worst performance. It is observed that rectangular and triangular have similar performances, inferior to circular (7,1) and superior to circular (4,4). Though rectangular outperforms triangular in PAPR performance, its minimum Euclidean distance is smaller. As a result of the combined influence of PAPR and minimum Euclidean distance, the performances of rectangular and triangular are similar. Considering the impact of bias voltage, the dynamic range of input signal vpp is smaller when the bias voltage is relatively lower or higher because of the severer nonlinearity compared with that under the optimal bias voltage. When the bias voltages are 1.8 and 2.3 V, circular (7,1) increases the dynamic range by 0.26 V, or about 200%, compared with circular (4,4). In addition, the dynamic range at 2.3 V is overall upward in order to maintain certain modulation depth. When the bias voltage is 2.0 V, the

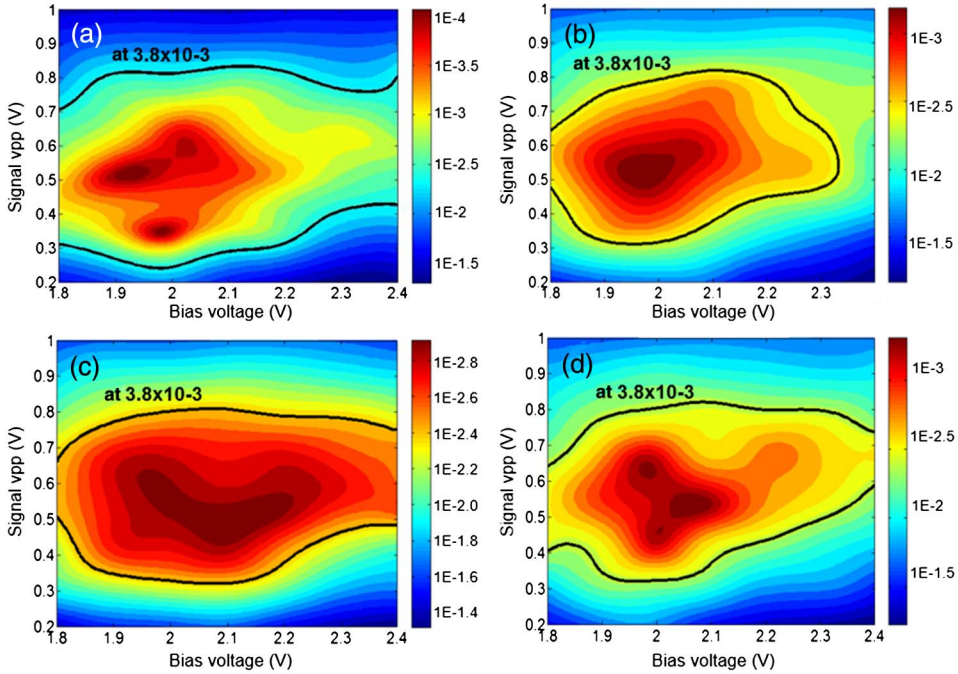

Fig. 8. BER versus different bias voltage and signal vpp for (a) circular (7,1), (b) circular (4,4), (c) rectangular, and (d) triangular.

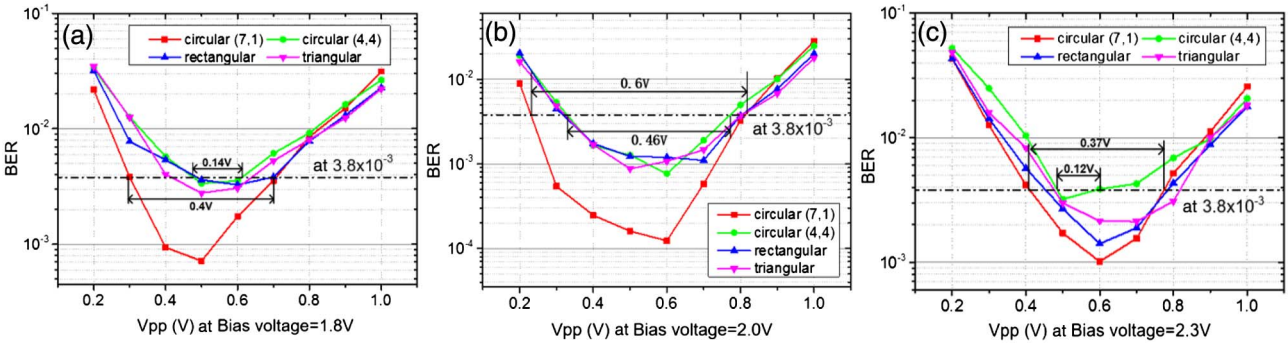

Fig. 9. BER versus signal vpp (a) at bias voltage = 1.8 V, (b) at bias voltage = 2.0 V, and (c) at bias voltage = 2.3 V.

Table 3. Dynamic Range of Signal VPP Under Different Bias Voltage

Constellation	**Circular (7,1)**		**Circular (4,4)**	
Dynamic range	V_Bias = 1.8 V	0.40 V (0.30 V–0.70 V)	V_Bias = 1.8 V	0.14 V (0.48 V–0.62 V)
	V_Bias = 2.0 V	0.60 V (0.22 V–0.82 V)	V_Bias = 2.0 V	0.46 V (0.32 V–0.78 V)
	V_Bias = 2.3 V	0.37 V (0.41 V–0.78 V)	V_Bias = 2.3 V	0.12 V (0.48 V–0.60 V)
Constellation	**Rectangular**		**Triangular**	
Dynamic range	V_Bias = 1.8 V	0.22 V (0.48 V–0.70 V)	V_Bias = 1.8 V	0.23 V (0.4 V–0.63 V)
	V_Bias = 2.0 V	0.48 V (0.32 V–0.8 V)	V_Bias = 2.0 V	0.46 V (0.32 V–0.78 V)
	V_Bias = 2.3 V	0.34 V (0.45 V–0.79 V)	V_Bias = 2.3 V	0.34 V (0.48 V–0.82 V)

increase is about 0.14 V, or 30%. The nonlinearity at 2.0 V is relatively slight so that the enhancement is not so obvious. In short, circular (7,1) provides a wider dynamic range, which is flexible in a more complicated working environment to meet the communication and lighting requirements.

Under the optimal bias voltage and signal vpp, we measured the Q factor and BER performance for different constellations at different baud rate over 1 m free space transmission. Figure 10 shows that circular (7,1) performs best; next is the rectangular, triangular comes in third, and the performance of circular (4,4) is the poorest. The results agree with the nonlinear resistance analysis but disagree with the noise-resistance analysis and high-frequency attenuation-resistance analysis in Section 2. It indicates that the system performance is dominated by the nonlinear effect. According to Fig. 10, with the increase of the baud rate, the enhancement of the Q factor is greater because the high-speed transmission system demands a higher sensitivity. At 500 MBd, circular (7,1) outperforms circular (4,4), with a Q-factor improvement of 4.5 dB. According to Fig. 11, only circular (7,1) can achieve the baud rate of 500 MBd and even higher under a BER threshold of 3.8×10^{-3}. Compared with circular (4,4), the highest baud rate of circular (7,1) is increased by 35 MBd, namely, 105 Mbit/s.

For a clearer comparison of the data rate enhancement, we measured the highest baud rate of the four special-shaped constellations at different transmission distances. Because of the cutoff frequency of 500 MHz of the PIN PD, the baud rate is limited around 500 MBd. According to the results shown in Fig. 12, the performance difference among the four constellations is generally similar to the previous results. Compared with circular (4,4), which has the poorest performance, circular (7,1) provides an improvement of 35 MBd, namely 105 Mbit/s at the distances of 0.5, 1, and 2 m; and 30 MBd, namely 90 Mbit/s at the distance of 1.5 m. What is

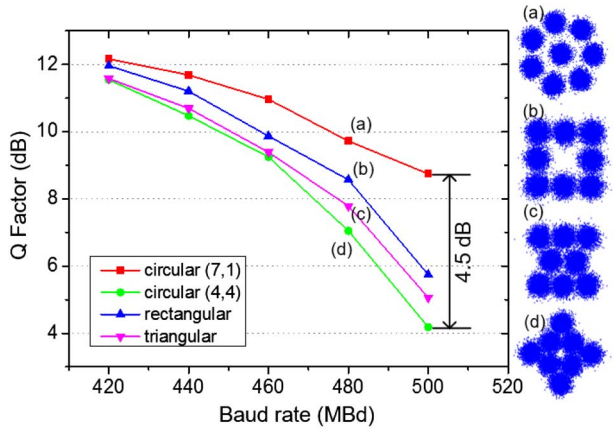

Fig. 10. Q-factor comparison for different 8-QAM constellations.

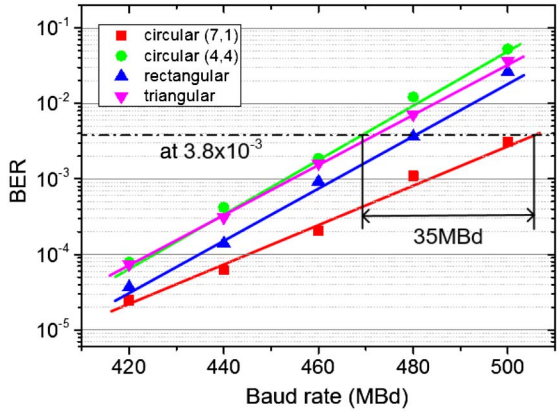

Fig. 11. Baud rate comparison for different 8-QAM constellations.

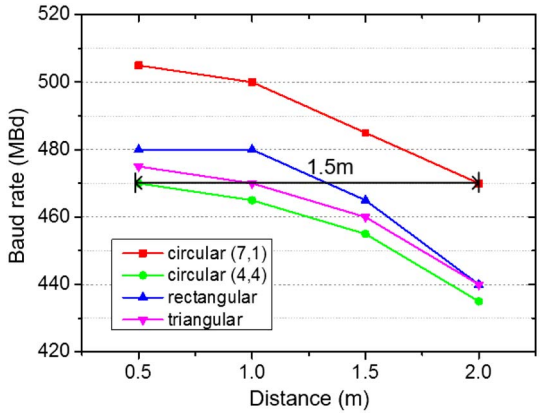

Fig. 12. Highest baud rate versus transmission for different 8-QAM.

more, when the baud rate is 470 MBd, the transmission distance of circular (7,1) is 1.5 m longer than that of circular (4,4). The highest baud rate, 505 MBd, is successfully achieved by circular (7,1) at the distance of 0.5 m. That is to say, the system capacity is up to 1.515 Gbit/s.

It is worth noting that our investigation of the constellation can be further extended to 4-QAM and 16-QAM. The higher level modulation will be a reasonable solution for future high-speed VLC systems. However, the constellations of higher QAM will be more sophisticated depending on different allocation schemes, such as triangular, rectangular, or circular allocation, which will result in different Euclidean distances. Furthermore, the high-order modulation will give more stringent limitation on the system nonlinearity. Therefore, the system performance of higher order QAM modulation with various constellations should be a critical problem for future investigations.

It should be noted that the VLC system in this experiment is subject to the limited bandwidth of the PIN PD with a cutoff frequency of 500 MHz. If the bandwidth of the receiver can be extended, further improvement of system capacity can be obtained, and the performance difference among the four special-shaped 8-QAM constellations will be more obvious. In addition, the transmission rate will be increased by several times if the green, blue, and amber chips are all utilized to carry information.

5. CONCLUSION

In this paper, for the first time, we report an experimental comparison of four special-shaped 8-QAM constellations in a single-carrier VLC system. The dynamic range of signal vpp at different bias voltages is investigated. When the bias voltage is lower or higher than the optimal bias voltage, the dynamic range is smaller due to the more serious signal distortion induced by the nonlinear relationship between the LEDs' forward current and driving voltage. In addition, among the four special-shaped 8-QAM constellations, circular (7,1) shows obvious superiority in dynamic range performance for its lower PAPR, which is able to satisfy more complicated communication and lighting demands.

Furthermore, by measuring the Q factor and the highest data rate of the system utilizing the four constellations, it is found that circular (7,1) is the optimum constellation and rectangular comes in second, then triangular; circular (4,4) is the worst choice. The results indicate that the experimental system is dominated by the nonlinear effect. Circular (4,4) is the most widely used 8-QAM constellation due to its simple generation with an IQ modulator, and, compared with circular (7,1), its slight weakness in anti-noise performance almost can be ignored. However, in a nonlinearity dominated system, its deficiency is amplified. Circular (7,1) outperforms circular (4,4) with a Q-factor improvement of 4.5 dB at 500 MBd. Besides, the highest data rate is increased by 105 Mbit/s, and the transmission distance is increased by 1.5 m at 470 MBd. The highest data rate of 1.515 Gbit/s is successfully achieved by circular (7,1) over 0.5 m free space transmission. But for the limited bandwidth of the receiver PIN, the performance gap between circular (7,1) and circular (4,4) will be more obvious. The results also indicate the research value of the application of circular (7,1) in orthogonal frequency division multiplexing modulation systems, where nonlinear effectiveness is more serious due to the higher PAPR.

In conclusion, it is experimentally demonstrated that circular (7,1) shows an absolute advantage in single-carrier VLC systems and is the most potential 8-QAM constellation appropriate for more complicated and stringent application scenarios. Moreover, the successful exploration of special-shaped 8-QAM constellations in single-carrier VLC systems inspires us to make further research on constellation-shaping schemes of higher order QAM signals in more complicated multicarrier systems.

Funding. National Natural Science Foundation of China (NSFC) (61571133), National "863" Program of China (2015AA016904).

REFERENCES

1. Y. Wang, Y. Wang, N. Chi, J. Yu, and H. Shang, "Demonstration of 575-Mb/s downlink and 225-Mb/s uplink bi-directional SCM-WDM visible light communication using RGB LED and phosphor-based LED," Opt. Express **21**, 1203–1208 (2013).
2. N. Chi, Y. Wang, Y. Wang, X. Huang, and X. Lu, "Ultra-high-speed single red-green-blue light-emitting diode-based visible light communication system utilizing advanced modulation formats," Chin. Opt. Lett. **12**, 010605 (2014).
3. D. Wu, W. D. Zhong, Z. Ghassemlooy, and C. Chen, "Short-range visible light ranging and detecting system using illumination light emitting diodes," IET Optoelectron. **10**, 94–99 (2015).
4. P. H. Pathak, X. Feng, P. Hu, and P. Mohapatra, "Visible light communication, networking, and sensing: a survey, potential and challenges," IEEE Commun. Surv. Tutorials **17**, 2047–2077 (2015).
5. C. Thomas, M. Weidner, and S. H. Durrani, "Digital amplitude-phase keying with M-ary alphabets," IEEE Trans. Commun. **22**, 168–180 (1974).
6. G. J. Foschini, R. D. Gitlin, and S. B. Weinstein, "Optimization of two-dimensional signal constellations in the presence of Gaussian noise," IEEE Trans. Commun. **22**, 28–38 (1974).
7. H. Kwok and D. Jones, "PAR reduction via constellation shaping," in *Proceedings of IEEE International Symposium on Information Theory* (IEEE, 2000), p. 166.
8. S. Sezginer and H. Sari, "Peak power reduction in OFDM systems using dynamic constellation shaping," in *13th European Signal Processing Conference*, September 2005, pp. 1–4.
9. A. Mobasher and A. K. Khandani, "Integer-based constellation-shaping method for PAPR reduction in OFDM systems," IEEE Trans. Commun. **54**, 119–127 (2006).
10. N. H. Tran and H. H. Nguyen, "Signal mappings of 8-ary constellations for bit interleaved coded modulation with iterative decoding," IEEE Trans. Broadcast. **52**, 92–99 (2006).
11. G. Hosoya and H. Yashima, "Constellation shaping for non-uniform signals in bit-interleaved coded modulation combined

with multi-stage decoding," in *Australian Communications Theory Workshop (AusCTW)*, (January 2016), pp. 181–186.
12. M. Nölle, F. Frey, R. Elschner, C. Schmidt-Langhorst, A. Napoli, and C. Schubert, "Performance comparison of different 8QAM constellations for the use in flexible optical networks," in *Optical Fiber Communication Conference*, (March 2014).
13. E. Agrell and M. Karlsson, "Power-efficient modulation formats in coherent transmission systems," J. Lightwave Technol. **27**, 5115–5126 (2009).
14. P. A. Bello and B. D. Nelin, "The effect of frequency selective fading on the binary error probabilities of incoherent and differentially coherent matched filter receivers," IEEE Trans. Commun. Syst. **11**, 170–186 (1963).
15. K. Ying, Z. Yu, R. J. Baxley, H. Qian, G. K. Chang, and G. T. Zhou, "Nonlinear distortion mitigation in visible light communications," IEEE Wireless Commun. **22**, 36–45 (2015).
16. W. Yan, B. Liu, L. Li, Z. Tao, T. Takahara, and J. C. Rasmussen, "Nonlinear distortion and DSP-based compensation in metro and access networks using discrete multi-tone," in *European Conference and Exhibition on Optical Communication*, (September 2012), pp. Mo-1.
17. X. Huang, Z. Wang, J. Shi, Y. Wang, and N. Chi, "1.6 Gbit/s phosphorescent white LED based VLC transmission using a cascaded pre-equalization circuit and a differential outputs PIN receiver," Opt. Express **23**, 22034–22042 (2015).